DELINEATION OF FAULT ASSISTED AQUIFER USING TRIPOTENTIAL WENNER ARRAY-TECHNIQUE AROUND ITA-ONIYAN INDUSTRIAL LAYOUT, AKURE, NIGERIA.

G. M. OLAYANJU
Department of Applied Geophysics, Federal University of Technology, P.M.B. 704, Akure, Nigeria

Abstract. Concealed fault assisted aquifer has been located by the tripotential resistivity survey with Wenner electrode configuration. The interpretations of data acquired were made in terms of comparison of the filtered and unfiltered Wenner alpha-apparent resistivity space sections, ratio profiles and computer aided qualitative interpretation of the alpha-apparent resistivity curves. The results of the study demonstrated that in order to be able to site borehole for underground water supply for both domestic and industrial uses in the study area, the well will have to be located along observed bedrock depression of high degree of fracturing, jointing and fissuring which will provide secondary porosity and permeability of the underlying crystalline bedrock. Although, high resistivity contrast of resistivity values at large electrode spacing seems to make the interpretation of the space sections and ratio sections difficult, filtered data however ensure a reasonable data integrity.

1. INTRODUCTION

Geophysicists usually employ the use of electrical resistivity methods in exploring for groundwater resource worldwide. The conventional Wenner vertical electrical depth sounding technique enjoys wide applications in lithological boundary differentiation, determination of subsurface water resource, subsurface geologic characteristics and determination of the nature of the superficial deposits [1,2,3,4,5,]

The use of non-conventional Wenner Tripotential-(α, β, and γ) apparent resistivity survey, as well as the ratio of beta-to-gamma apparent resistivity $\rho_a^\beta / \rho_a^\gamma$ ratio provide means of distinguishing between the effects of lateral and vertical resistivity variations [6,7].

In time past, significant efforts have been made by institutions and individuals to find suitable locations for groundwater boreholes for portable water supply for industrial and residential purpose within Ita-Oniyan community and its environs in the Northwestern part of Akure.

Major problems being encountered in the area arise from the clayey nature of the underlying weathered rocks constituting the regolith. Occurrence of elevated outcrops of solid rocks such as charnokite, granite, and low lying biotite gneiss coupled with the thick section of clayey regolith make it difficult to locate a suitable location for portable groundwater boreholes.

Hand-dugged wells within flooding areas and places close to river channels are the only source of groundwater for domestic purposes. Existence of abortive wells in Cooperative Federation Limited (area of this investigation) and at a nearby Ondo State Radio-vision Corporation (OSRC) premises, suggest that only fault-assisted aquifer or fractured bedrock can produce high yield deep-boreholes needed to meet both residential and industrial yearning for suitable groundwater in this area of study.

The present research then employs the use of non-conventional tripotential resistivity methods to delineate subsurface lithological units, presence of superficial deposit and bedrock features such as faulting, fracturing, lineaments and determination of degree of fracturing anisotropy in the study area.

This work is expected to provide information on hydrogeological significance of the geoelectric parameters (i.e., layer resistivity values and thickness), lithologic differentiation, and the use of beta-to-gamma apparent resistivity ratio to assess the subsurface geometry and delineation of geologic condition such as occurrence of fault/fractured zones within the study area.

2. SITE HISTORY AND GEOLOGICAL BACKGROUND

The area of investigation is situated in the northwestern part of Akure, Ondo State, Nigeria (Fig. 1). The area of study constitutes the part of Ita-Oniyan community, hosting the Akure Northwestern Industrial layout, which is situated along Akure-Owo expressway and falls within latitude 7° 17^{l} N to 7° 17.8^{l} N and longitude 5° 10^{l} E and 5° 10.5^{l} E (Fig. 2).

The rocks of the Precambrian complex of the southwestern Nigeria underlie the area [8,9,10]. Underlying lithological units mainly comprise Charnokite and Biotite. Outcrops of the solid rocks of Charnokite with maximum peak of about 396m forming rugged hilly environment and low-lying Biotite gneiss are common in the Northwestern and

Nig. J. Pure & Appl. Phys (2003) Vol.2 pp 6-15. Printed in Nigeria, ISSN 1596-0862.Email: njpap@futa.edu.ng For rights of reproduction and web access, contact African Jounals Online, UK. www.inaps.ajol.

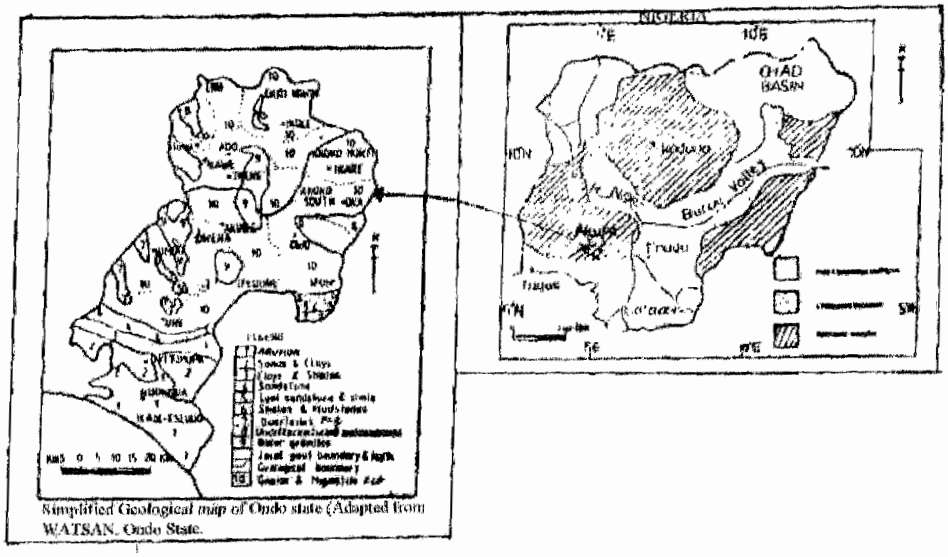

Fig. 1 Location map of Ondo State, Nigeria. (Modified from Olayanju and Adelusi, 2002)

Southwestern parts of the area [11]. Other outcrops include quartzite and granite. The surface elevation ranges from 372m to 396m above mean sea level (AMSL). The land cover of the area of investigation is about 25,000m^2 with gently sloppy and undulating topography. Previous geophysical works carried out within the premises of the Food processing industrial building in the industrial layout, such as geological mapping of the area, evidence from the road cuttings and deep degree of chemical weathering at the surface close to the abortive wells, show that the concealed bedrock is Charnokitic [11,12]. In some areas reddish to brown (dense and hardened) ferruginous weathered material and boulders reflect the deep effects of chemical weathering at the surface.

3. GEOPHYSICAL SURVEY

The geophysical survey involved the use of both tripotential profiling and vertical electrical sounding techniques using the Wenner electrode configurations. Three traverses (AA$^{|}$, BB$^{|}$, and CC$^{|}$) were arbitrarily established parallel to each other along NW-SE direction (see Fig. 2). Traverse CC$^{|}$ was actually planned close to BB$^{|}$, based on the suspected lateral local resistivity variations observed along traverse CC$^{|}$, where a surface occurrence of a highly altered Gneiss-boulder was encountered.

Four VES stations were occupied along traverse AA$^{|}$, while a total of five VES stations were occupied on traverse BB$^{|}$. The inter-electrode spacing 'a' varies between 1m to 64m for the VES stations, except at VES 1 where the maximum electrode spacing of 96m was attained. The electrode spreads were oriented in N070°E geographic azimuth direction.

The vertical triple α-, β-, and γ- apparent resistivity measurements were presented as depth sounding curves (triple apparent resistivity curves) and space sections. Quantitative interpretations of the simple depth problems in terms of the geoelectric parameters (layer thickness and resistivity values) of a layered earth were carried out through partial curve matching of the α-apparent resistivity curve aided by the computer iteration based on the Ghosh linear filtering theory [13].

Typical triple α-, β-, and γ- apparent resistivity curves obtained from the field data and respective depth interpretations of the α- apparent resistivity configuration are shown in Figs. 3 and 4, and Table 1. Geoelectric sections were also produced from the obtained geoelectric parameters.

Tripotential horizontal profiling using Wenner configuration with constant electrode spacing of 20m was carried out along traverse CC$^{|}$ in the N290°E geographic azimuth.

The geophysical traverse having a lateral coverage of 210m covers effectively the zone of the presumed near surface lateral resistivity variations. Tripotential horizontal profiling measurements and values of the ratio $\rho_a^{\beta} / \rho_a^{\gamma}$ at

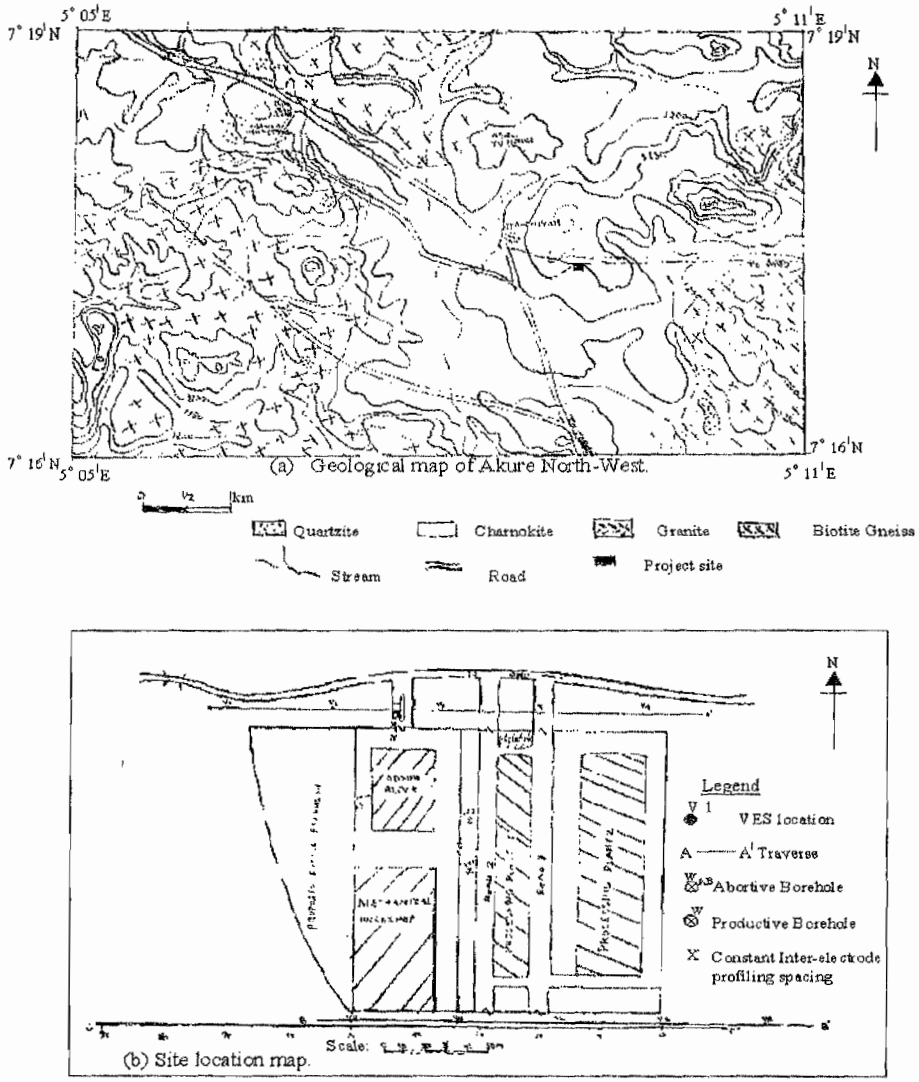

Fig. 2 Location and Geological maps of Ita-Oniyan, Northwestern part of Akure, Nigeria. (Adapted from Olayanju, 1995).

constant electrode spacing of 20m were presented as the triple apparent resistivity profiles and ratio profile respectively (Fig. 5). The equipment used for the geophysical survey was the PASI-E2 digital tetrameter along with Taylor BK-85 electrode swooper which facilitated electrode array switch into the three α-, β-, and γ- apparent resistance measurement modes during the field operations.

4. DISCUSSION OF RESULTS

4.1 Triple apparent resistivity curves

The observed tripotential responses to the lateral changes in the earth resistivity are demonstrated as shown on the typical triple apparent resistivity curves (Fig. 3) for the various surface VES locations. The effect of the surface concretion of the lateritic topsoil (hard pan) at VES locations 3 and 4 on traverse AA' and that of stations 5, 6 and 7 on traverse BB' can easily be observed on these curves.

However the persistence of the spurious effects due to the existence of possibly dipping fault at large electrode spacing beneath VES locations 2 and 3 on traverse AA', 6 to 7 on traverse BB' are very evident of the triple apparent resistivity curves. These same effects are also observable on the space sections discussed below.

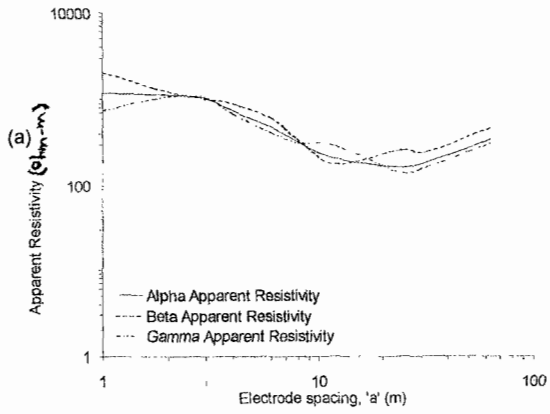

VES 3

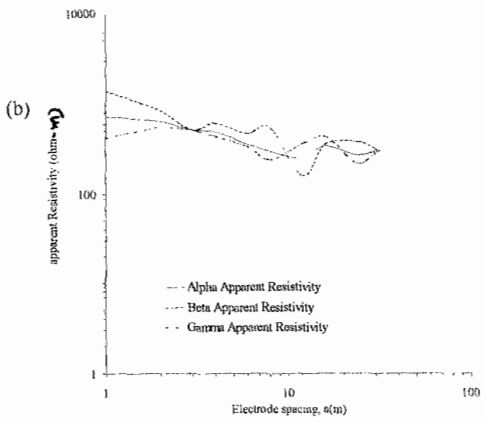

VES 4

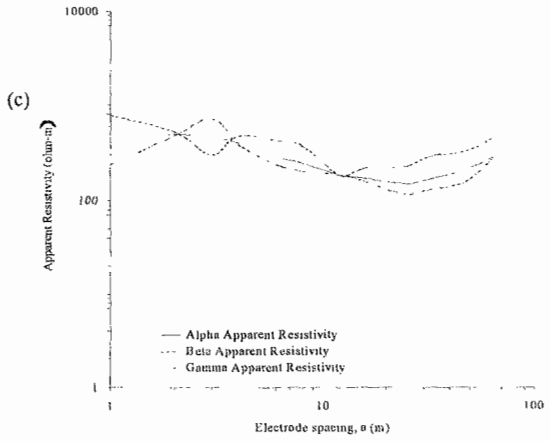

VES 5

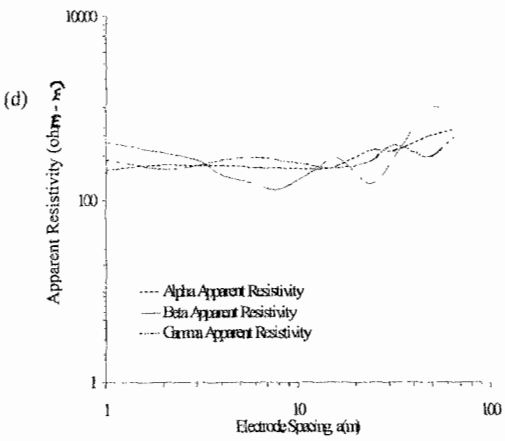

VES 6

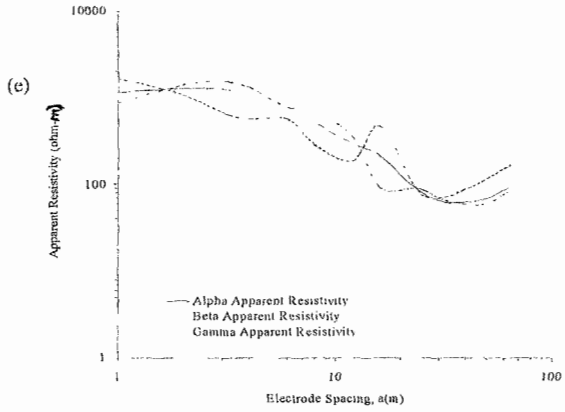

VES 7

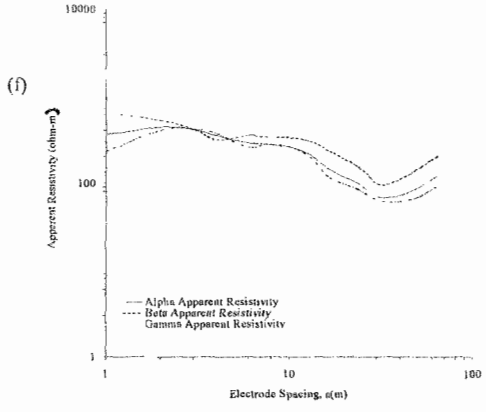

VES 8

Fig. 3 Triple-Apparent Resistivity Curves at various VES locations. (Both evidences of the near surface effect of the lateritic hardpan and dipping fault interface extending to a deeper depth could be easily seen on the curves).

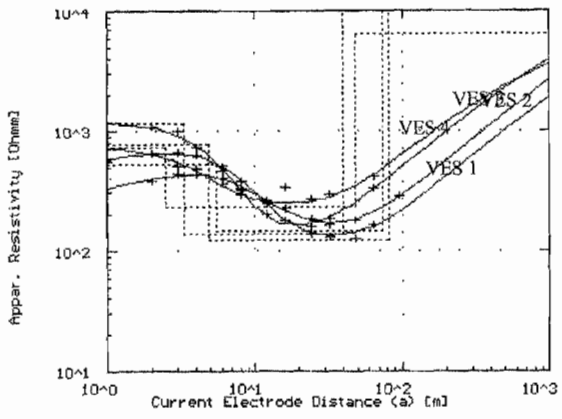

(4a) Vertical Electrical Sounding Curves for traverse AA'.

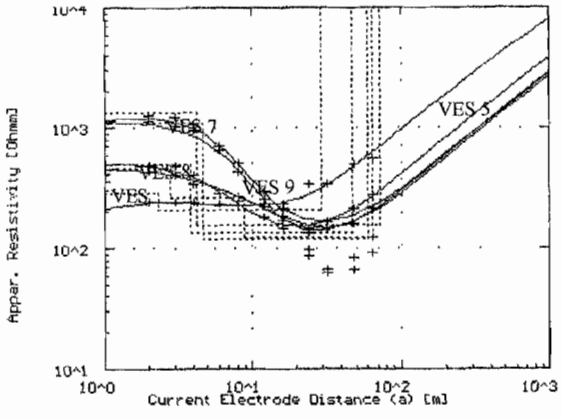

(4b) Vertical Electrical Sounding Curves for traverse BB'.

Fig. 4 Wenner α-apparent resistivity sounding curves of the study area.

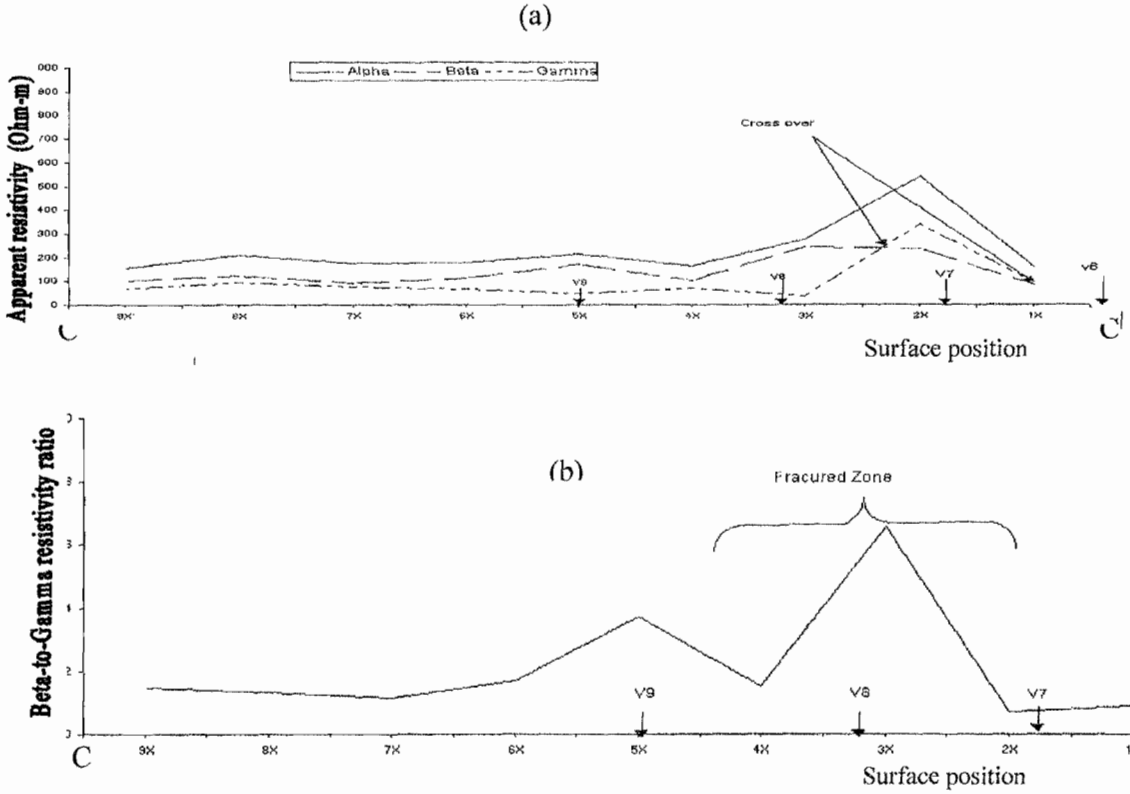

Fig. 5 (a) Wenner tripotential constant separation profile at X = 20m. (b) The ratio of $\rho_a^{\beta}/\rho_a^{\gamma}$ plotted against Wenner electrode separation X =20m.

As demonstrated by Worthington and Baker [14], initial comparison of R_α with $R_\beta+R_\gamma$ at large electrical spacings usually exceeds 10% and persists beneath the profile in the E-W directions. Originally on the acquired data, the spurious effect is less observable at small electrode spacing, which actually comes from the occurrence of very hard lateritic topsoil in some area.

Obtained α-, β- and γ- apparent resistivity data were eventually filtered based on the Ghosh linear filter [13] and that of expanded offset filter of Acworth and Griffiths [15]. The filtered α-apparent resistivity curves were quantitatively interpreted to provide the layer resistivity and thickness of the lithologic units shown by the two-geoelectric sections (see Fig. 8).

Comparison of the lithologic columns provided through the interpreted VES results with that of bore hole logs of the wells drilled in the area of study indicated a high degree of correlation.

4.2 Tripotential profiling and ratio profiles

The tripotential profiling carried out along profile CC^1, made at about 0.5m away from profile BB^1 was made to verify the observed lateral resistivity anomaly presumed to have been due to the occurrence of a faulted bedrock depression. The tripotential profile section (Fig. 5) indicates the fracture zone with a dipping plane. It was observed that the ratio values of the $\rho_a^\beta / \rho_a^\gamma$ are relatively less than unity over and around the areas of the outcropped gneiss boulder between VES stations 6 and 7, an indication of increase in resistivity with depth at a shallow level here. Over the fractured zone, there was a sharp change in the ratio (between 3.76 and 6.56), while over the remaining parts of the profile the changes in geoelectric parameters follow a normal trend and value slightly above unity. The decrease in apparent resistivity values is indicated by the value of $\rho_a^\beta / \rho_a^\gamma$ which is greater than unity and this actually supports the occurrence of the fractured basement constituting the aquifer in this area.

Evaluation of the fractured coefficient of anisotropy λ was made using Dar Zarrouk parameters [1,16,17] of traverse resistance T and longitudinal conductance S, using the relation

$$\lambda = (T * S)^{1/2} / H \qquad (1)$$

where $T = \sum_{hi} \rho_i$, $S = \sum_{hi} / \rho_i$, and $H = \sum_{hi}$. h_i and ρ_i are the thickness and resistivity of the respective layers.

It has been observed that low λ values and low layer resistivity usually characterized rocks with low primary porosity, while high values of λ normally correspond to development of secondary porosity within a rock exhibiting macroanisotopy (generally fracture anisotropy) diagnostic of hydraulic conductivity [18]. Olorunfemi et al., [16] has observed that high anisotropy coefficient (usually greater than 1.2) and relatively low weathered layer resistivity value that are less than 150 ohm-m are associated with mica schist, while λ values less than 1.2 and relatively high weathered layer resistivity greater than 150 ohm-m are characteristic of gneiss (granite gneiss, biotite gneiss and banded gneiss) of the Western basement of Nigeria.

The values of coefficient of anisotropy observed in the study area were found to fall between 1.0 and 1.24 (see table 1). λ values of 1.17, 1.23 and 1.24 were obtained at VES locations 7, 3 and 9 with respective weathered layer resistivity values of 153 ohm-m, 138 ohm-m and 120 ohm-m. These values could only be attributed to the development of secondary porosity arising from the fractured bedrock in the area, as indicated by their high bedrock resistivity values, which are characteristic of gneiss (or sometimes charnokitic gneiss). It is then clear from the observed coefficient of anisotropy values that the study area will be lying within the geologic boundaries between the charnokite in the west and the granite gneiss in the east.

4.3 Tripotential Space sections

Figures 6 and 7 show the obtained Wenner Alpha space sections by plotting the unfiltered α-apparent resistivity at depth approximate by the normalized depth of investigation (NDI) of 0.5a as derived by Edwards [19]. The ratio sections of $\rho_a^\beta / \rho_a^\gamma$ were plotted at depth of 0.6a as obtained by Acworth and Griffiths [15].

The laterally changing ratio clearly indicates lateral variations in the resistivity values, especially prominent over the lateritic topsoil at VES location 4 and omitted station X over profile AA^1. As the ratio values are greater than unity in most portions of the profiles a decrease in resistivity with depth is indicated at respective NDIs. It was also inferred, (and later confirmed by the borehole data), that the bedrock is usually deep and dips within the area. On the other hand the Wenner space sections and the ratio sections show an event believed to be characteristic of fault beneath VES stations 3, 2, 6, 7 and 8. It was inferred that fault plane is shallow beneath locations 3,2 and 6, while it extends to greater depth at other locations 7 and 8. This suggests the existence of fractured zones extending through the basement into the fresh bedrock. It is then believed that there is network of connected fractures and joints within a bedrock depression that is clearly supported by the exceptionally high yield at well 1 location.

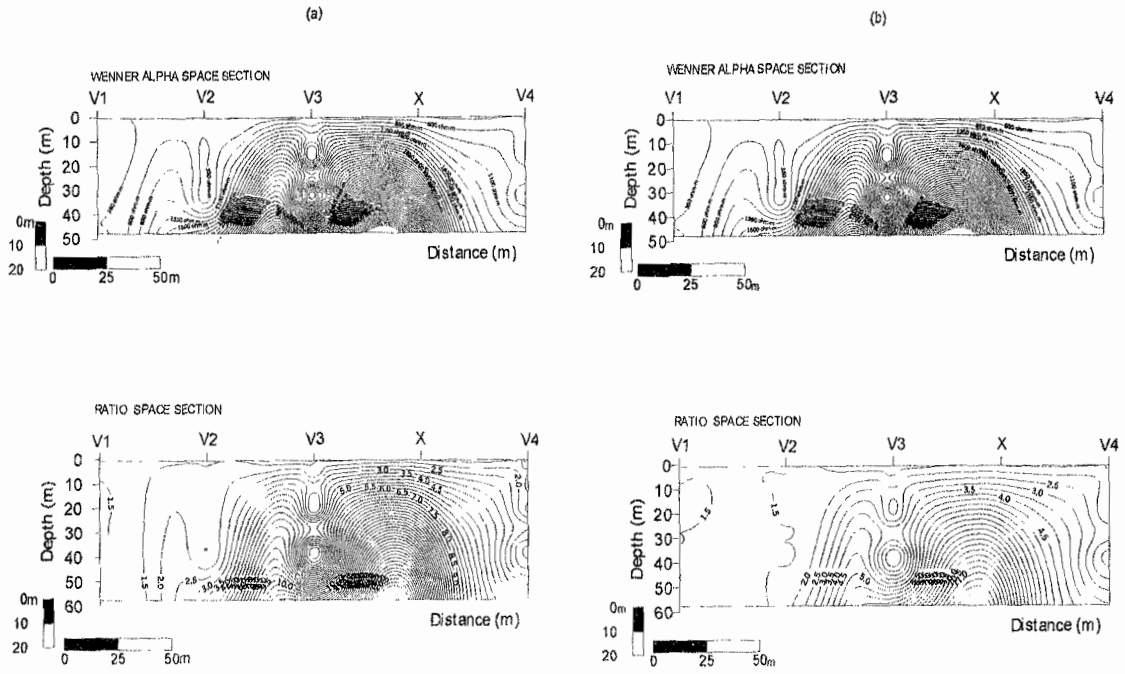

Fig. 6 (a) Unfiltered α-apparent resistivity section and $\rho_a^{\beta}/\rho_a^{\gamma}$ ratio section, (b) α-apparent resistivity section and $\rho_a^{\beta}/\rho_a^{\gamma}$ ratio section of the filtered data along profile AA$^{|}$.

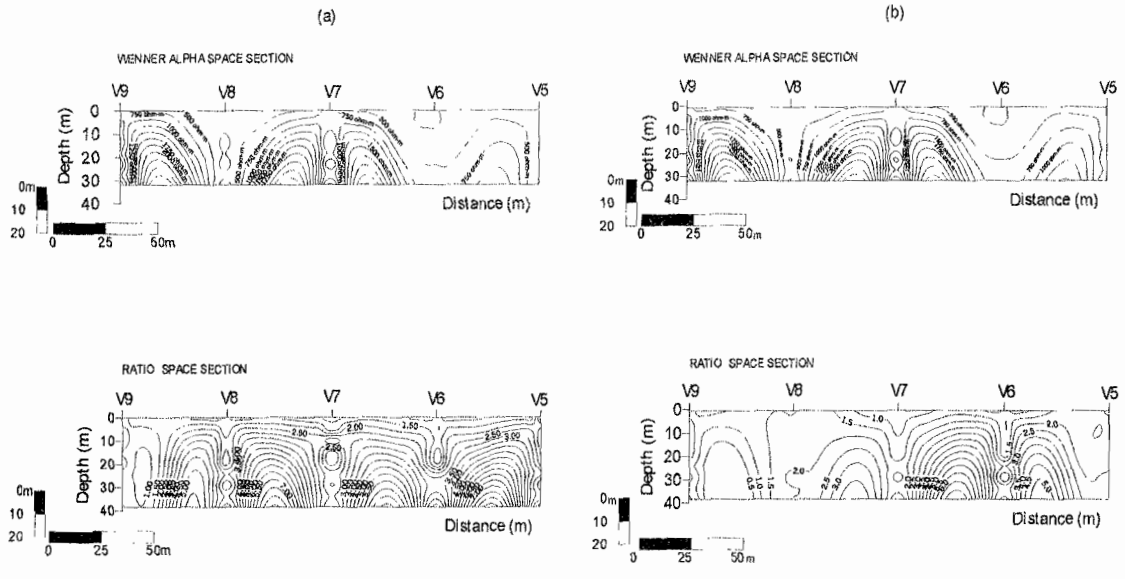

Fig.7 (a) Unfiltered α-apparent resistivity section and $\rho_a^{\beta}/\rho_a^{\gamma}$ ratio section, (b) α-apparent resistivity section and $\rho_a^{\beta}/\rho_a^{\gamma}$ ratio section of the filtered data along profile BB$^{|}$.

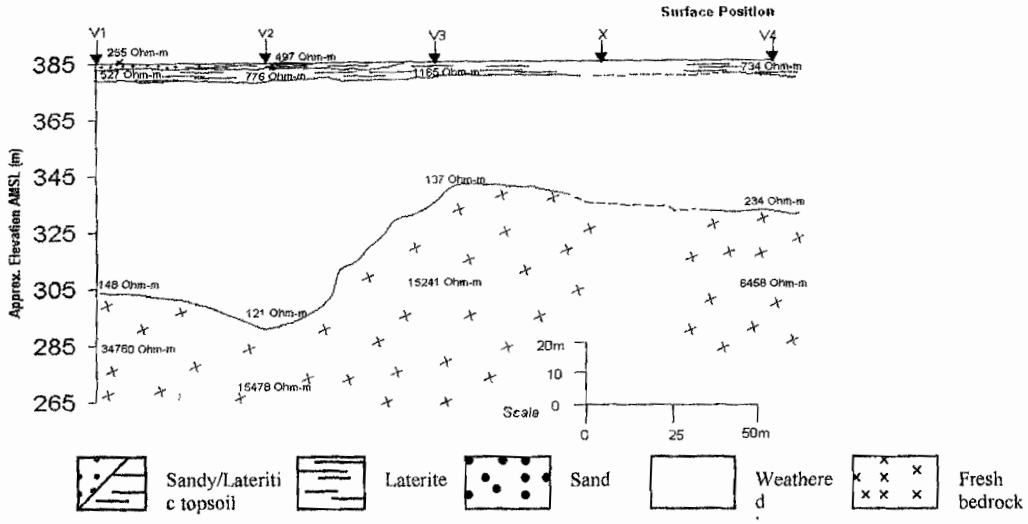

Fig. 8 (a) Geoelctric section along profile AA'.

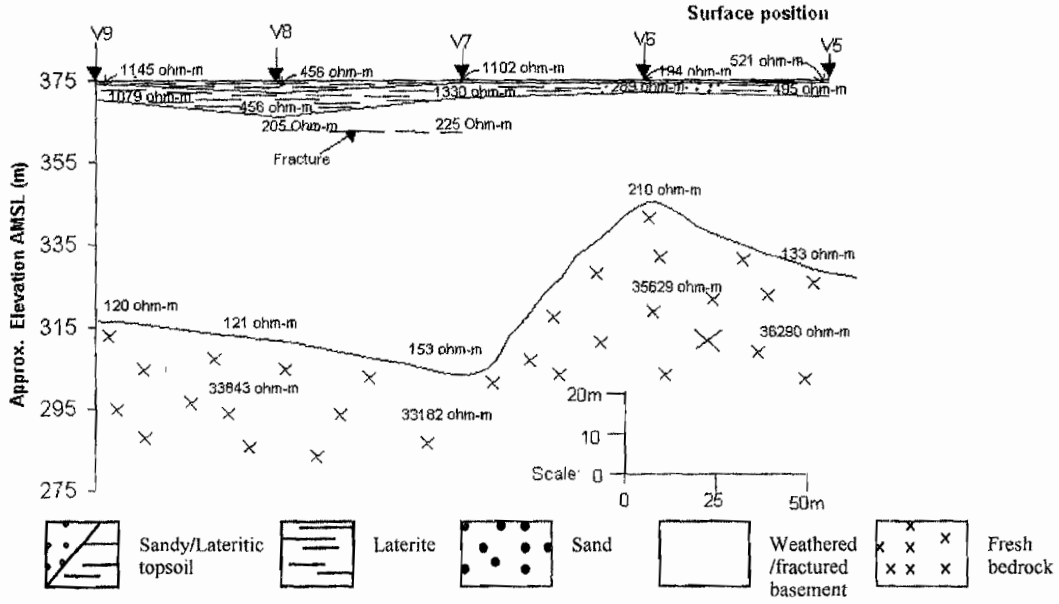

Fig. 8 (b) Geoelctric section along profile BB'.

4.4 Geoelectric sections

Two geoelectric sections (Fig. 8) were produced from the interpreted α- apparent resistivity configuration of the triple-apparent resistivity curves. The geoelectric sections demonstrate the occurrence of maximum four layers and minimum of three layers within the study area. 3-layer curves were only observed at VES locations 3 and 4 where the topsoil is composed of hard concretion of the laterite at the surface.

The first layer has the resistivity values between 194 ohm-m and 1165 ohm-m, which are diagnostic of sandy to lateritic topsoil, having thickness ranging from 0.5m to 3.3m. The second layer mostly lateritic is characterized by layer resistivity values between 138 ohm-m and 1330 ohm-m. This layer graduates from laterite in the upper part to sandy materials down dip in the North-south direction. The first and second layers could be grouped together as the topsoil as the borehole logs indicated (Fig. 9). The topsoil thickness and depth to the weathered layer are not well defined on the borehole logs. The Thickness of the second layer was estimated to vary between 1.5m to 5.9m. The layer was absent at VES locations 3 and 4.

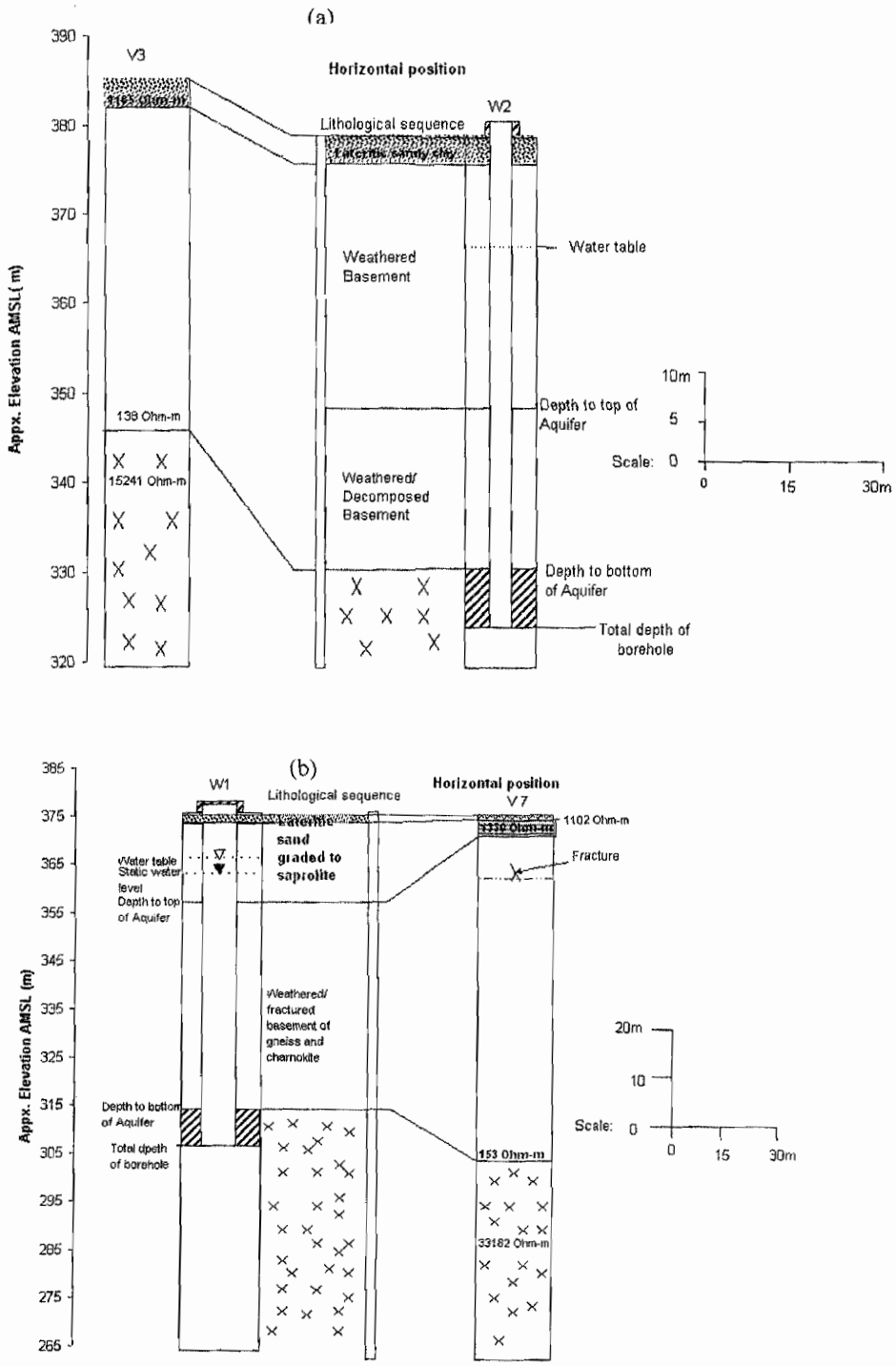

Fig. 9: Correlation of the borehole Lithologic logs and the wells along the dip direction in the study area.

Table 1: Summary of layer parameters (Computer iteration results and coefficient of anisotropy values)

	Layer	1	2	3	4	Coefficient of anisotropy
VES 1	Res. (ohm-m)	255	527	148	34760	$\lambda = 1.01$
RMS_Err = 1.1 %	Thick (m)	0.7	4.8	69.1	-	
VES 2	Res. (ohm-m)	4978	776	121	15478	$\lambda = 1.11$
RMS_Err = 1.1 %	Thick (m)	0.7	4.1	77.2	-	
VES 3	Res. (ohm-m)	-	1165	138	15241	$\lambda = 1.23$
RMS_Err = 1.1 %	Thick (m)	-	3.3	36.2	-	
VES 4	Res. (ohm-m)	-	733.9	234	6458	$\lambda = 1.04$
RMS_Err = 1.1 %	Thick (m)	-	2.5	45.7	-	
VES 5	Res. (ohm-m)	521	495	133	36290	$\lambda = 1.07$
RMS_Err = 1.1 %	Thick (m)	0.5	3.3	42.9	-	
VES 6	Res. (ohm-m)	194	289	210	35629	$\lambda = 1.0$
RMS_Err = 0.9 %	Thick (m)	0.8	1.5	27.1	-	
VES 7	Res. (ohm-m)	1102	1130	153	33182	$\lambda = 1.17$
RMS_Err = 1.4 %	Thick (m)	0.8	3.4	67.7	-	
VES 8	Res. (ohm-m)	456	262	121	33843	$\lambda = 1.07$
RMS_Err = 0.9 %	Thick (m)	2.8	5.9	54.6	-	
VES 9	Res. (ohm-m)	1145	1079	120	38679	$\lambda = 1.24$
RMS_Err = 2.1 %	Thick (m)	0.8	3.8	54.2	-	

However, the third layer comprising the fractured/weathered constituting the aquifer has resistivity values ranging from 120 ohm-m to 234 ohm-m, and thickness between 27.1m to 77.2m, the highest value was observed at VES location 2. The bedrock depression in the area has a SE-NW direction trending towards the valley in the western part of the study area, while the general fault trend is fairly NE-SW in orientation. The fourth layer that forms the bedrock is characterized by resistivity values between 6458 ohm-m and 38680 ohm-m. The lowest value observed at VES locations 4 is presumed to be due to development of macroanisotropy (fracture anisotropy) at greater depth of the bedrock.

5. CONCLUSION

The results of this study have demonstrated the importance of tripotential resistivity method in delineating fracture anisotropy (or inhomogeniety) of crystalline basement rocks which may be attributed to structural elements like foliation, joints and fractures which will eventually lead to high well yields. The low weathered basement resistivity (less than 240 ohm-m) and intense fracturing observed in the study area were adduced to be responsible for high yield of a particular well in the area. It was then realized that in order to locate areas suitable for drilling of water supply wells the position of the wells needs to lie along established fault assisted bedrock depressions, since the area is characterized by rocks having low primary permeability and low porosity.

The use of the tripotential method in this way has provided significant information on the subsurface geometry and hydrogeological importance of the localized fault assisted aquifer unit in the area.

Acknowledgements

The author wishes to thank Professor S.L. Folami for his moral supports. Also, I wish to express my sincere gratitude to Mr. A.O. Adelusi for suggestions and for reviewing the manuscript.

REFERENCES

1. Zohdy, A.A.R. (1974): Electrical methods in application of surface geophysics to groundwater investigations. Techniques of water resources investigations of the United States, Geological Survey Book 2, Chapter D1, pp. 47-55.
2. Van Overmeeren, R.A. (1981): A combination of electrical resistivity, seismic refraction and gravity measurement of groundwater exploration in Sudan. Geophysics, Vol. 46, No. 6, pp. 1304-1311.
3. Palacky, G.J. (1989): Resistivity characteristics of Geologic Targets. In M.N. Babighion, Ed., Electromagnetic methods in Applied Geophysics, Vol. 1 (Theory) IG, No. 3. SEG, pp. 53-129.
4. Keary, P., and Brooks, M. (1996): An introduction to Geophysical Exploration. 2nd Ed., Blackwell science Ltd., London.
5. Olayanju, G.M., and Adelusi, A.O. (2002): Geoelectric Characteristic Study and its Hydogeologic Implications of Iyange Area, Northwestern Part of

Akure, Nigeria"; J. of Appl. Sci. Vol. 5, No. 4. (in press).

6. Carpenter, E.W. (1955): Some notes concerning the Wenner configuration. Geophysical Prospecting, Vol. 3, pp. 388-402.
7. Carpenter, E.W., and Haberjam, G.M. (1956): A Tripotential method of Resistivity prospecting. Geophysics, Vol. XXI, No.2, pp.455-469.
8. Boesse, J.M. (1988): A geological map of Obafemi Awolowo University campus. Unpublished.
9. Olorunfemi, M.O., and Okhue, E.T. (1992): Hydrogeologic and geologic significance of a geoelectric survey at Ile-Ife, Nigeria. Jour. Min. Geol., Vol. 28, No. 2, pp. 221-229.
10. Folami, S.L. (1998): Geological and geophysical mapping of Precambrian rocks in Odo-igbo area of Osun state, southwestern Nigeria. AMSE journal, Vol. 57, No. 1, pp. 1-24.
11. Olayanju, G.M. (1995): Tripotential Studies of the Area around Ondo State Cooperative Federation Limited, Owo-Ilesa Way, Akure. Unpublished B. Tech. Applied Geophysics Thesis, Federal University of Technology, Akure, Nigeria.
12. Ojo, J.S., Folami, S.L., and Olorunfemi, M.O. (1993): Predrilling geophysical survey for ground water development in the premises of Coop Cocoa Products Ltd., Akure. (Technical report). 13pg.
13. Ghosh, D.P. (1971): Inverse filter coefficient for the computation of apparent resistivity standard curves for horizontal stratified earth. Geophysical prospecting, vol. 19, pp. 761-775.
14. Worthington, P.F., and Baker, R.D. (1977): Detection of disused vertical mineshaft at shallow depths by geoelctrical methods. Geoexploration, Vol. 15, pp. 111-120.
15. Acworth, R.I., and Griffiths, D.H. (1985): Simple data processing of tripotential apparent resistivity measurements as an aid to the interpretation of subsurface structure. Geophysical prospecting, Vol. 33, pp. 861-887.
16. Olorunfemi, M.O., Olarewaju, V.O., and Alade, O. (1991): On the electrical anisotropy and groundwater yield in a Basement Complex area of SW Nigeria. JAES, Vol. 12, No.3, pp. 467-472.
17. Okurumeh, O.K., and Olayinka, A.I. (1998): Electrical anisotropy of crystalline Basement rocks around Okeho, southwestern Nigeria: Implications in geologic mapping and ground water investigation. Jour. of NAH, Vol. 9, pp.41-50.
18. Watson, K. A., and Barker, R.D. (1999): Differentiating anisotropy and lateral effects using azimuthal resistivity offset Wenner soundings. Geophysics, Vol. 64, No. 3, pp. 739-745.
19. Edwards, L.S. (1977): A modified pseudosection for resistivity and induced-polarization. Geophysics, Vol. 42, pp. 1020-1036.